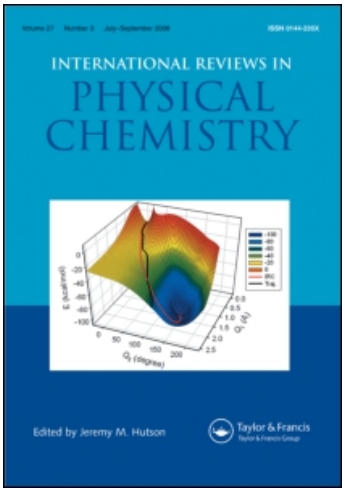

International Reviews in Physical Chemistry
Publication details, including instructions for authors and subscription information:
http://www.informaworld.com/smpp/title~content=t713724383

Fixed-node quantum Monte Carlo

James B. Anderson[a]
[a] Department of Chemistry, The Pennsylvania State University, University Park, Pennsylvania, USA

To cite this Article Anderson, James B.(1995) 'Fixed-node quantum Monte Carlo', International Reviews in Physical Chemistry, 14: 1, 85 — 112
To link to this Article: DOI: 10.1080/01442359509353305
URL: http://dx.doi.org/10.1080/01442359509353305

INTERNATIONAL REVIEWS IN PHYSICAL CHEMISTRY, 1995, VOL. 14, NO. 1, 85–112

Fixed-node quantum Monte Carlo

by JAMES B. ANDERSON

Department of Chemistry, The Pennsylvania State University, 152 Davey Laboratory, University Park, Pennsylvania 16802, USA

Quantum Monte Carlo methods cannot at present provide exact solutions of the Schrödinger equation for systems with more than a few electrons. But, quantum Monte Carlo calculations can provide very low energy, highly accurate solutions for many systems ranging up to several hundred electrons. These systems include atoms such as Be and Fe, molecules such as H_2O, CH_4, and HF, and condensed materials such as solid N_2 and solid silicon. The quantum Monte Carlo predictions of their energies and structures may not be 'exact', but they are the best available. Most of the Monte Carlo calculations for these systems have been carried out using approximately correct fixed nodal hypersurfaces and they have come to be known as 'fixed-node quantum Monte Carlo' calculations. In this paper we review these 'fixed node' calculations and the accuracies they yield.

1. Introduction

Most quantum chemists are aware that quantum Monte Carlo methods have proved remarkably successful in providing accurate predictions of energies and structures for molecular systems containing a few electrons. The first quantum calculation to achieve an absolute accuracy of 1·0 microhartree for a polyatomic system was a quantum Monte Carlo calculation [1] for the H_3^+ molecular ion. The first to achieve an accuracy of 0·01 kcal mol^{-1} in the potential energy surface for the reaction $H + H_2 \rightarrow H_2 + H$ was a quantum Monte Carlo calculation [2]. The first to achieve an absolute accuracy of 0·1 K for the dimer He–He was a quantum Monte Carlo calculation [3] 12 000 times more accurate in absolute energy than the lowest-energy analytic variational calculation. For these systems and for other systems of a few electrons, such as LiH [4], HeH [5], and H_2 [6], quantum Monte Carlo methods can provide solutions of the time-independent Schrödinger equation without systematic error [7].

For larger systems neither quantum Monte Carlo methods not analytic variational methods can at present provide such exact' results. However, for many of these larger systems quantum Monte Carlo calculations provide the lowest-energy, most accurate results available. The systems include atoms such as Be [8] and Fe [9], molecules such as H_2O [10], CH_4 [11], and HF [12], and condensed materials such as solid N_2 [13] and solid silicon [14]. The quantum Monte Carlo results for these systems may not be 'exact', but they are the best available. Most of the Monte Carlo calculations for these systems have been carried out using approximately correct fixed nodal hypersurfaces and they have come to be known as 'fixed-node quantum Monte Carlo' calculations. The purpose of this review is to make quantum chemists aware of these 'fixed-node' calculations and the accuracies they yield for systems ranging from a few electrons to several hundred electrons.

The fixed-node method is the first of several methods available for incorporating the effects of particle indistinguishability in quantum Monte Carlo calculations [15, 16].

0144–235X/95 $10·00

For systems of electrons it allows the introduction of the Pauli exclusion principle by the specification of nodal hypersurfaces in the configuration space of the electrons separating that space into positive and negative regions such that the overall wavefunction is antisymmetric to the exchange of electrons. It is thus one solution to the 'sign problem in fermion Monte Carlo'. Since the nodal hypersurfaces are not specified by symmetry except in special cases, they cannot in general be specified exactly except by complete solution of the problem. However, approximately correct nodal hypersurfaces may be obtained from approximate solutions, and the use of such 'fixed-nodes' in quantum Monte Carlo calculations can lead to highly accurate solutions.

In this chapter we review the fixed-node quantum Monte Carlo method, a little bit of its history, its formulation, its positive and negative aspects, and its prospects for further development. We also review its applications. These now include more than one hundred studies of molecular systems large and small as well as condensed-matter systems.

We begin with a description of the diffusion quantum Monte Carlo method (DQMC) for the solution of the many-electron Schrödinger equation and continue with a discussion of the related Green function quantum Monte Carlo method (GFQMC). We then outline the characteristics of nodal hypersurfaces for atomic and molecular wavefunctions, their use in fixed-node calculations and some of the practical considerations required for the successful implementation of these calculations before proceeding to the applications.

2. Diffusion quantum Monte Carlo

The diffusion quantum Monte Carlo method of solving the time-independent Schrödinger equation consists of a simple game of chance involving the random walks of particles through space and their occasional multiplication or disappearance. It is based on the similarity between the Schrödinger equation and the diffusion equation (i.e., Fick's second law of diffusion) and the use of the random walk process to simulate the diffusion process. The equivalence of the two equations was noted as early as 1932 by Wigner [17]. A random walk simulation of the Schrödinger equation was suggested by Fermi in the 1940's and was discussed by Metropolis and Ulam [18] and by King [19] in 1949. A number of related techniques were proposed and discussed in succeeding years, but it was not until fast computers became available that applications to multicentre chemical systems became practical [15].

The equation to be solved is the time-independent Schrödinger equation,

$$H\Psi = E\Psi, \tag{1}$$

or

$$-\sum_i \frac{\hbar^2}{2m_i}\nabla_i^2\Psi(X) + V(X)\Psi(X) = E\Psi(X), \tag{2}$$

where the summation is over the electrons or other particles i having masses m_i and the nomenclature is standard. For simplicity we consider the equation for a single particle of mass m, rearranged to become

$$\frac{\hbar^2}{2m}\nabla^2\Psi(X) - V(X)\Psi(X) = -E\Psi(X). \tag{3}$$

The equation has as solutions the wavefunctions $\Psi_0(X)$, $\Psi_1(X)$, ... which exist only for specific energies E_0, E_1, ...

The wavefunction may be treated as a function of an additional variable τ defined according to

$$\Psi(X,\tau) = \Psi(X)\exp(-E\tau), \tag{4}$$

The function then behaves according to

$$\frac{\partial\Psi(X,\tau)}{\partial\tau} = -E\Psi(X,\tau), \tag{5}$$

and we have

$$\frac{\partial\Psi}{\partial\tau} = \frac{\hbar^2}{2m}\nabla^2\Psi - V\Psi. \tag{6}$$

The function $\Psi(X, \tau)$ in (6) may be considered general, but at large values of τ its solution is given by the $\Psi(X,\tau)$ of (4) corresponding to the lowest-energy or ground-state wavefunction for the system. Since the higher states decay faster according to (4) an arbitrary initial function consisting of a sum of terms containing the wavefunctions for the ground-state and any or all the higher states decays to the ground-state wavefunction. The arbitrary initial function evolves to the ground-state solution of the time-independent Schrödinger equation.

Because of its similarity to the time-dependent Schrödinger equation, (6) is often referred to as the Schrödinger equation in imaginary time. The analogy is formally correct since solutions of the time-dependent Schrödinger equation have equivalent real and imaginary parts under steady-state conditions.

The Schrödinger equation in imaginary time τ has the same form as the diffusion equation with an added first-order reaction term,

$$\frac{\partial C(X,t)}{\partial t} = D\nabla^2 C(X,t) - kC(X,t). \tag{7}$$

The concentration C corresponds to the wavefunction Ψ, the diffusion coefficient D corresponds to the group $\hbar^2/2m$, and the rate constant k corresponds to the potential energy V.

Differential equations are normally used to model the behaviour of physical systems and the diffusion equation above is normally used to model the behaviour of a system in which particles undergo diffusion by a random walk process. In quantum Monte Carlo calculations the random walk process is used to simulate the differential equation. Of course, the connection between the random walk process and quantum mechanics may be considered to be direct. In the absence of the Schrödinger equation one might still use the Monte Carlo method to obtain solutions to quantum mechanical problems, but the connection between random walks and quantum mechanics is most easily made with the aid of the Schrödinger equation as above.

The random walk process and the diffusion equation are related through the diffusion coefficient by the Einstein equation [20],

$$D = \frac{\overline{(\Delta x)^2}}{2\Delta\tau}, \tag{8}$$

which gives the diffusion coefficient for particles moving a distance Δx at random positive or negative at intervals of time $\Delta\tau$. In the simulation of the Schrödinger equation in imaginary time the time and distance steps are chosen to produce the appropriate value of D (or $\hbar^2/2m$) given by (8).

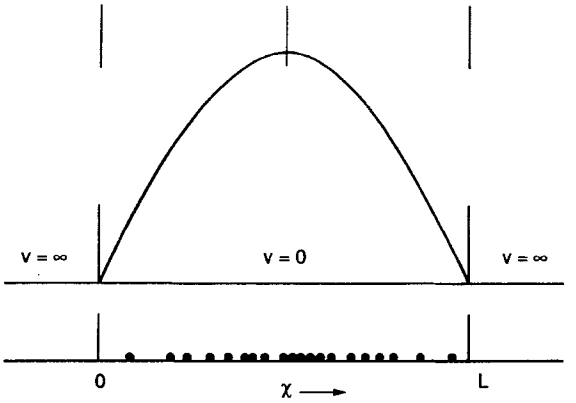

Figure 1. Illustration of the diffusion quantum Monte Carlo method for the problem of the particle-in-a-box.

The standard quantum mechanical problem of the particle in a one-dimensional box serves to illustrate the diffusion quantum Monte Carlo method. The box is illustrated in figure 1. The potential energy inside the box, within the region $0 < x < L$, is zero. Outside the box, for $x < 0$ and $x > L$, the potential energy is infinity. An initial collection of particles, typically called 'walkers' or 'psi-particles' or 'psips' in order to distinguish them from the 'particle-in-the-box', is distributed in the region $0 < x < L$. Time is advanced one step $\Delta\tau$. To simulate the diffusion term of (7) each psip is moved right or left at random a distance Δx. To simulate the multiplication term of (7) each psip then gives birth to a new psip with a probability $P_b = -V\Delta\tau$ if V is negative or disappears with a probability $P_d = V\Delta\tau$ if V is positive. Time is advanced another step and the process is repeated. If the number of psips falls below an acceptable lower limit or increases beyond an acceptable upper limit, their number may be adjusted by the random multiplication or removal of psips present. (Caution: In making such adjustments one must be very careful to avoid introducing any bias.) For the particle-in-a-box as specified psips diffuse to the walls and disappear on encountering the infinite potential energy, but they are replaced by psips multiplying within the box. After a large number of iterations the distribution of psips approaches a fluctuating 'steady-state' distribution—the function $\sin(\pi x/L)$—which corresponds to the wavefunction for the ground state of the particle in the box.

The game is readily extended to problems having a higher number of dimensions and is clearly most useful for problems in which the number of dimensions is large. A system of n electrons free to move in three dimensions each can be simulated by a collection of psips moving in $3n$ dimensions each.

The first application of the DQMC method to molecular systems was made in our laboratory [15] with a calculation of the energy of the H_3^+ molecular ion. The Schrödinger equation in imaginary time for the two-electron H_3^+ system with three nuclei fixed is given, in atomic units by

$$\frac{\partial \Psi}{\partial \tau} = \tfrac{1}{2}\nabla_1^2\Psi + \tfrac{1}{2}\nabla_2^2\Psi - V\Psi. \tag{9}$$

With the electrons labelled 1 and 2 and the three protons labelled A, B, C the potential

energy V, exclusive of internuclear terms, is

$$V = -\frac{1}{r_{1A}} - \frac{1}{r_{1B}} - \frac{1}{r_{1C}} - \frac{1}{r_{2A}} - \frac{1}{r_{2B}} - \frac{1}{r_{2C}} + \frac{1}{r_{12}}, \tag{10}$$

in which r_{1A} is the distance between electron 1 and proton A and so forth. It is convenient to introduce a reference potential V_{ref} so that the operating equation becomes

$$\frac{\partial \Psi}{\partial \tau} = \tfrac{1}{2}\nabla_1^2\Psi + \tfrac{1}{2}\nabla_2^2\Psi - (V - V_{\text{ref}})\Psi. \tag{11}$$

In terms of the diffusion equation we then have $D = 1/2$ and $k = (V - V_{\text{ref}})$.

The random walk in six dimensions was executed with non-uniform step sizes in each dimension selected from a Gaussian distribution with probabilities P of step sizes Δx given by

$$P(\Delta x) = \frac{1}{(2\pi)^{1/2}\sigma} \exp\left[-\frac{(\Delta x)^2}{2\sigma^2}\right]. \tag{12}$$

The probability of birth was given by $P_b = -(V - V_{\text{ref}})\Delta\tau$ for $(V - V_{\text{ref}})$ less than zero and the probability of disappearance was given by $P_d = (V - V_{\text{ref}})\Delta\tau$ for $(V - V_{\text{ref}})$ greater than zero. After each move a random number in the interval (0, 1) for each psip was compared with P_b (or P_d) and if smaller than P_b (or P_d) then a birth (or death) was completed.

The calculations were begun with a collection of 1000 psips in positions corresponding to electron configurations in the region of the nuclei. A large time step was used for a rapid approach to a steady-state distribution. The step size was decreased as time progressed and fixed at a small value to improve the accuracy of the results in the accumulation of data after steady-state was reached.

In order to maintain the number of psips approximately constant the arbitrary reference potential V_{ref} was adjusted at the end of each time step. (To avoid bias, a large delay prior to adjustment is advised.) At steady-state the energy E corresponding to a wavefunction Ψ may be evaluated using (5) rearranged as

$$E = -\frac{1}{\Psi}\frac{\partial \Psi}{\partial \tau}. \tag{13}$$

For a given distribution the wavefunction is proportional to the total number of psips N and one has

$$E = -\frac{1}{N}\frac{\partial N}{\partial \tau}. \tag{14}$$

In the case of the ground state of H_3^+, which has no boundaries serving as sinks or sources for psips, the total number of psips is not directly affected by the diffusion terms of (9) but changes according to

$$\frac{\partial N}{\partial \tau} = -\sum_N (V - V_{\text{ref}}). \tag{15}$$

The energy was thus given by the average potential energy $\overline{V}$ according to

$$E = \overline{V}. \tag{16}$$

After steady-state was reached the energies at each time step were retained for a subsequent determination of the overall average for a large number of samples.

There are five important sources of error in these first diffusion Monte Carlo calculations: (*a*) statistical or sampling error associated with the limited number of

independent sample energies used in determining the energy from an average of variable potential energies, (*b*) the use of a finite time-step $\Delta\tau$ rather than an infinitesimal time-step as required for the exact simulation of a differential equation, (*c*) numerical error associated with truncation and/or round-off in computing, (*d*) imperfect random number quality, (*e*) failure of the distributions to reach the steady-state or equilibrium distributions in a finite number of steps. Sources (*c*), (*d*), and (*e*) are common problems in computing. They can be detected relatively easily and eliminated, and they were not found to limit the calculations in any significant way. Sources (*a*) and (*b*) seriously limited the accuracy of the early calculations for H_3^+. The energy for this nodeless system was found to be $-1{\cdot}343$ hartrees, and the uncertainty in that energy, due largely to a combination of time-step error and statistical error, was $\pm 0{\cdot}013$ hartrees. Twenty years of refinement of methods, together with faster computers, has reduced that uncertainty by a factor of 13 000 to $\pm 0{\cdot}000\,001$ hartree [1].

For systems containing two or more electrons of the same spin or other indistinguishable particles, an additional problem appears: the node problem. For these systems it is necessary to restrict the form of the total wavefunction (space and spin parts) such that it is antisymmetric to the exchange of electrons. For any electronic state other than the ground state it is necessary to restrict further the properties of the wavefunction. The effect of these restrictions is the imposition of nodal surfaces, on which $\Psi(X) = 0$, in the space part of the wavefunction. For systems of a few electrons—H_2 [6], H–H–H [2], He–He [3], H–He [5]—the node problem can be overcome by exact cancellation methods [21] and 'exact' solutions (i.e., solutions free of systematic error) can be obtained. For systems of as many as ten electrons [22] released-node or transient-estimate methods can provide excellent approximate solutions. But, in general, the method of choice for systems of more than about ten electrons is the fixed-node method. Although the fixed-node method is variational in nature and does not yield exact results, it is the only choice available for quantum Monte Carlo calculations on many larger systems. The fixed-node method is remarkably accurate, and it generally yields energies well below those of the best available analytic variational calculations.

3. Green function quantum Monte Carlo

For certain boundary conditions the diffusion equation may be solved with the use of standard Green function methods, and the diffusion equation with an added first-order reaction term may be treated by these methods. The Green function quantum Monte Carlo method is similar to the DQMC method but takes advantage of the properties of Green functions in eliminating time-step entirely in treating the steady-state equation. The GFQMC method makes possible very large step sizes, but some of the advantages of large steps are lost for fixed-node calculations. The Green function quantum Monte Carlo method was proposed by Kalos [23] for nodeless systems. Procedures for introducing fixed nodes were developed later.

The time-independent Schrödinger equation, (3), may be written in the form

$$-\nabla^2\Psi(X) + k^2\Psi(X) = k^2\frac{V(X)}{E}\Psi(X), \tag{17}$$

where

$$k^2 = -\frac{2mE}{\hbar^2}. \tag{18}$$

To keep k^2 positive the energy must be made negative. This can be done by adjusting the reference or zero of the potential energy by an appropriate offset of energy.

The Green function for (17) which satisfies the boundary conditions for a problem in electronic structure (i.e., $\Psi \to 0$ as $X \to \infty$) is known and is given by

$$G(X, X') = \frac{1}{(2\pi)^{3N/2}} K_{3N/2-1}(k|X - X'|)/(k|X - X'|)^{3N/2-1}, \tag{19}$$

where K_ν is the modified Bessel function of the second kind.

The Green function method is carried out iteratively with steps analogous to time steps. Repetitive sampling is based on the property of the Green function which reproduces the wavefunction from itself,

$$\Psi(X) = \int G_0(X, X') \frac{V(X')}{E} \Psi(X') \, dX'. \tag{20}$$

The repeated application of (20) to an initially arbitrary wavefunction $\Psi(X')$ produces a wavefunction $\Psi(X)$ which is the lowest-energy solution to the Schrödinger equation for the boundary conditions specified. A psip in the distribution $\Psi(X')$ may be transferred to the distribution $\Psi(X)$, by multiplying its weight by $V(X')/E$, sampling the Green function distribution $G_0(X, X')$, and moving the psip to its new position X. Repetition for an initially arbitrary collection of psips leads to a set of psips which is a sample of points from the lowest-energy wavefunction for the boundary conditions and any other constraints imposed. As in DQMC the calculations must be carried out until a 'steady-state' distribution is obtained and sampling is carried out by continuing the calculations.

The imposition of additional boundaries corresponding to nodes for fixed-node calculations has been described by Ceperley [24], by Skinner *et al.* [25], and by Moskowitz and Schmidt [26]. The procedures involve conditional sampling together with smaller steps for psips in the vicinity of the nodes.

4. The fixed-node method

The fixed-node method was proposed in our 1975 paper [15] on diffusion quantum Monte Carlo and was immediately attacked as being inadequate [27]. We were, of course, aware of its limitations and recognized that exactly correct nodal hypersurfaces could not be obtained except from complete solutions of the Schrödinger equation. By the time our first paper appeared in print we had obtained rather good approximate results using the fixed-node method for several small systems—H ^{2}P, H_2 $^3\Sigma_u^+$, H_4 $^1\Sigma_g^-$, Be ^{1}S [16].

The fixed-node method is most easily illustrated for the case of the first excited state of a particle in a two-dimensional rectangular box. The wavefunction for the first excited state has a nodal surface which is a line dividing the region into two sections—one in which the wavefunction is positive and the other in which the wavefunction is negative—as shown in figure 2 (*a*). The wavefunction is zero at the nodal line. For electronic systems one knows something about the symmetry of the wavefunction: it is antisymmetric to the exchange of electrons of opposite spin. Let us suppose one knows something similar about the symmetry of the first excited state of the particle in the box: it is antisymmetry to inversion through the centre of the box. A wavefunction having that antisymmetry could have one of the nodal lines illustrated in figure 2 (*b*) as well as the correct nodal line shown in figure 2 (*a*). Any one of those lines has the required symmetry and could serve as a nodal line for a wavefunction with inversion

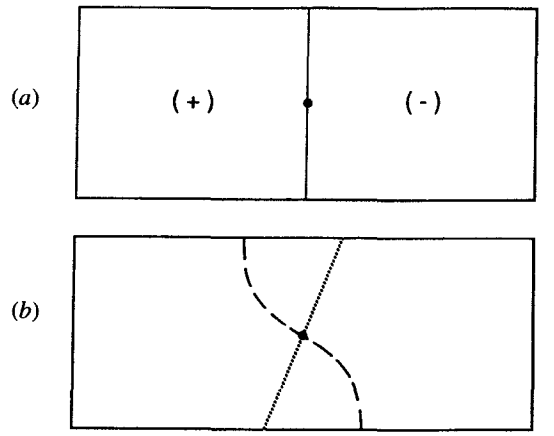

Figure 2 Nodal lines for the first excited state of a particle in a two-dimensional rectangular box. In (*a*) the correct node line is shown by the solid line. In (*b*) possible fixed-node lines of inversion symmetry, for a wavefunction with antisymmetry to inversion, are shown by dotted and dashed lines.

symmetry. A diffusion Monte Carlo calculation can be carried out with an assumed nodal line serving as a boundary along which the wavefunction is zero. The boundary divides the overall space into two regions of the same shape so that one calculation is sufficient to determine the wavefunction and energy for both. The Schrödinger equation is solved exactly within the boundaries.

Unless the assumed nodal surface is exactly correct the overall wavefunction will not be exactly correct and the energy obtained will be an upper bound to the true energy. The fixed-node method is thus variational with respect to node locations. If the nodes are wrong the calculated energy will be higher than the true energy. (Otherwise, an analytic variational calculation would yield a wavefunction having incorrect nodes and an energy lower than the true energy.) Nevertheless, it is our experience and the experience of others that wavefunctions having nodes which are approximately correct yield excellent energies. Approximately correct nodal surfaces are most readily available from approximately correct wavefunctions provided by analytic variational calculations.

Fixed-node calculations may be carried out using the simple diffusion quantum Monte Carlo procedure described above. The nodal surface typically divides the configuration space into identical regions such that a calculation in only one region is required. The boundary condition of $\Psi = 0$ at the nodal surface is enforced by eliminating (killing) any psip which diffuses across a node. Energies may be calculated from the growth rate as described above using (14), but (16) is not applicable since psips may disappear at the boundaries.

The molecule H_2 in its triplet state $^3\Sigma_u^+$ was one of the first molecules to be treated using the fixed-node quantum Monte Carlo method and it serves as a simple example. It has two electrons of like spin and a single nodal surface of five dimensions in the six-dimensional configuration space of the electrons, but because of symmetries the nodal surface is easily illustrated. The early variational calculations of James, Coolidge, and Present [28] give a fairly good energy and a reasonably accurate wavefunction for an internuclear distance of 1·6 bohrs. Their calculations were made with a number of approximate wavefunctions of increasing complexity and flexibility.

In figure 3 we reproduce plots of two of these functions made for our earlier discussion [16]. The nodal structures are shown by two series of plots in which the positions of the two nuclei and the first electron are fixed and the sign of the wavefunction is indicated according to the position of the second electron. For the functions used by James, Coolidge, and Present [28] this sign is a function only of the position of the second electron along the axis of the molecule and its radial distance from the axis. Thus, the two-dimensional plots of figure 3 are adequate to indicate the nodal surface. We note that there is a very significant difference in the nodal structures of the two variational wavefunctions. For the wavefunction identified as F there is much more curvature than for the wavefunction identified as H. Near the centre of the system for function F and over a large region for function H the nodal structure resembles a planar structure for which $\Psi = 0$ for $z_1 = z_2$ where z_i is the distance along the axis for electron i. The variational calculation for function H gives a slightly lower energy than that for function F.

Fixed-node calculations [16] for H_2 $^3\Sigma_u^+$ at an internuclear separation of 1·4 bohrs were carried out using a nodal surface given by $\Psi = 0$ for $z_1 = z_2$ as suggested by the plots of figure 3. The calculations were performed with different values for the time step using a modified version of the basic procedure designed to reduce the time-step error. The results are reproduced in figure 4. The values obtained for the energy, $-0{\cdot}7851 \pm 0{\cdot}0036$ hartrees at a time step of 0·010 atomic units and $-0{\cdot}7799 \pm 0{\cdot}0041$ hartrees at a time step of 0·020 atomic units were in excellent agreement with the value of $-0{\cdot}7831$ hartrees obtained in analytic variational calculations by Kolos and Roothaan [29]. A more accurate value from more recent calculations is $-0{\cdot}7842$ hartrees [30].

Early fixed-node calculations [31] were made for the H_4 square and helped to resolve an apparent conflict between experiment and theory on the mechanism for the four-body exchange reaction $H_2 + D_2 \rightarrow HD + HD$. Experimental measurements of the rate of reaction by Bauer and Ossa [32] and by a number of other workers [33] indicated an activation energy of 35–45 kcal mol^{-1} and rate expressions consistent with a direct bimolecular mechanism. Analytic variational calculations by Wilson and Goddard [34], Rubinstein and Shavitt [35], Silver and Stevens [36] and others predicted barrier heights of 115 kcal mole^{-1} or greater for a variety of bimolecular reaction paths. There appeared to be no explanation of the experimental results other than a bimolecular reaction, but the analytic predictions appeared to exclude that possibility. Any doubts about the accuracies of the analytic calculations had to be centred on possible inadequacies in the basis sets used. The basis sets for the variational calculations were all similar. The fixed-node quantum Monte Carlo calculations, for several different nodal surfaces derived from analytic variational calculations, gave nearly identical results and indicated a barrier no lower than 120 kcal mole^{-1}. This independent conclusion, reached without the use of a basis set, gave increased confidence in the theoretical predictions. Eventually, the earlier interpretations of the experiments were found to be in error and the observed results were attributed to reactions involving oxygen contaminating the system.

For the H_4 square in the $^1B_{1g}$ state the energy calculated with a nodal surface taken from a variational calculation with a single-zeta basis set was lower than the expectation value of the energy calculated with the same basis set. For the H_4 square in the $^1B_{1g}$ state the energy calculated using the simplest nodes meeting the symmetry requirements was found to be 65 kcal mole^{-1} below the expectation value of the energy for a double-zeta basis set. This general pattern is not at all unusual for comparisons of

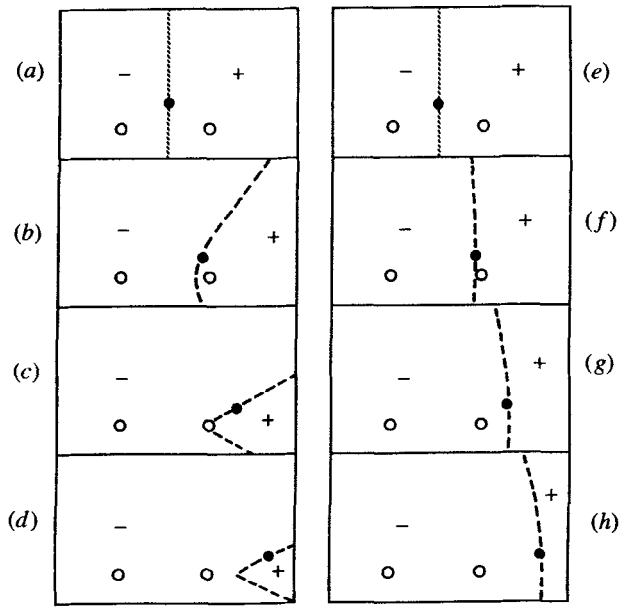

Figure 3. Node locations in calculations of James, Coolidge, and Present [28] for H_2 $^3\Sigma_u^+$. The protons are indicated by open circles, the first electron by a filled circle, and the node by a dashed line. Function F: (*a*)–(*d*). Function H: (*e*)–(*h*). The sign of the wavefunction is indicated according to the position of the in its triplet state second electron. From Anderson [16].

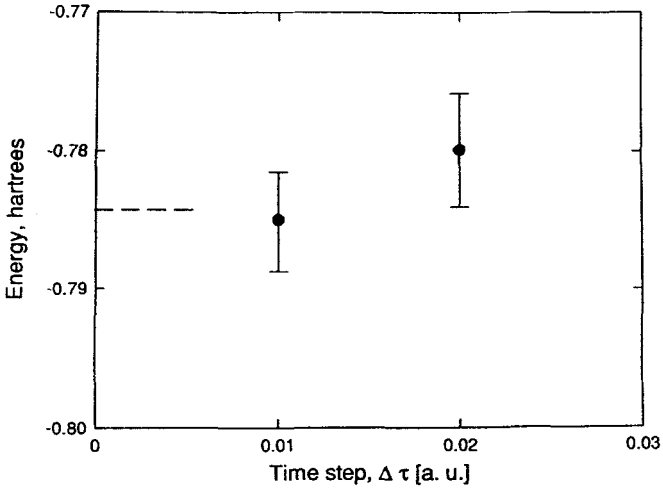

Figure 4. A fixed-node calculation for H_2 $^3\Sigma_u^+$. The exact value for the energy is indicated by the dashed line. From Anderson [16].

quantum Monte Carlo results with analytic variational results for small molecular systems. The total energies are usually significantly lower for the QMC calculations, and the relative energies—those yielding barrier heights, potential energy curves, and similar features of potential energy surfaces—are usually in fairly good agreement. This is the sort of behaviour one should expect when both types of calculations are correct within the accuracy expected.

5. Importance sampling for reduced variance

In principle, one should be able to take advantage of prior knowledge of the properties of wavefunctions to make quantum Monte Carlo calculations more efficient. Such prior knowledge is available in the form of wavefunctions from analytic variational calculations at several levels of approximation. It is possible to obtain very high accuracies by extending diffusion quantum Monte Carlo calculations to calculate corrections to trial wavefunctions rather than the complete wavefunction [37]. Repeated calculations produce successive corrections of smaller size and greater detail, but the method is not easily extended to large systems. Another means for variance reduction, now called 'importance sampling', was introduced by Grimm and Storer [38] in 1971. It is now the most widely used and most successful means for improving the accuracies of diffusion and Green function QMC calculations.

To obtain the importance-sampling version of diffusion quantum Monte Carlo, we first multiply the basic equation, (6), by a trial wavefunction Ψ_t and define a new term $f = \Psi\Psi_t$ which is the product of the true wavefunction and the trial wavefunction. After considerable rearrangement we obtain the basic equation for diffusion QMC with importance sampling,

$$\frac{\partial f}{\partial \tau} = \frac{\hbar^2}{2m}\nabla^2 f - \nabla\cdot(f\nabla \ln \Psi_t) - E_{\text{loc}} f. \tag{21}$$

The equation has terms on the right side corresponding to diffusion of psips with a diffusion coefficient of $\hbar^2/2m$, a drift term with a velocity given by $\nabla \ln \Psi_t$, and a first-order rate term for the disappearance of psips with a rate constant given by the local energy $E_{\text{loc}} = H\Psi_t/\Psi_t$ for the trial wavefunction.

In diffusion QMC the simulation of (21) is carried out in the same way as the simulation of (6) except that additional psip movement is required by the drift term and psip multiplication depends on the local energy rather than the potential energy. If the trial function is simply a constant the drift term is zero, the local energy is equal to the local potential energy, and the expression reduces to that for diffusion without importance sampling.

The nature of the drift term is such as to produce a drift of psips in the direction of higher Ψ_t. The psips are thus concentrated in the more important regions and their distribution, if Ψ_t is accurate, approximates that of Ψ^2, the square of the true wavefunction. In the vicinity of a nodal surface the velocity, which may be written as $\nabla\Psi_t/\Psi_t$, is increased and as Ψ_t approaches zero at the nodal surface, the drift velocity approaches infinity in a direction away from the surface. Psips are thus prevented from crossing the nodes of the trial function.

The computation procedure for diffusion with drift is similar to that of the basic random walk procedure described above. At each time step the values of $E_{\text{loc}} = H\Psi_t/\Psi_t$ and the drift velocity $\nabla \ln \Psi_t$ must be determined from the potential energy and from the first and second derivatives of the trial wavefunction. The drift distance is given by

the product of the vector drift velocity and the time step. Multiplication is based on the local energy.

A calculation generates a distribution of psips with a concentration corresponding to the value of the function $f = \Psi\Psi_t$. For the determination of energies an average of local energies is used. Following Grimm and Storer [38] one can obtain the expression giving the energy as the average of local energies for the f-particles or psips. Multiplying the time-independent Schrödinger equation by the trial function we obtain at any point

$$\Psi_t H\Psi = \Psi_t E\Psi. \tag{22}$$

Integrating over all space yields

$$\int \Psi_t H\Psi \, dX = \int \Psi E \Psi_t \, dX. \tag{23}$$

The Hermitian properties of wavefunctions, for identical boundary conditions and symmetries, allow a permutation to yield

$$\int \Psi H\Psi_t \, dX = \int \Psi E \Psi_t \, dX, \tag{24}$$

which may be rewritten as

$$\int \Psi\Psi_t \frac{H\Psi_t}{\Psi_t} \, dX = E \int \Psi\Psi_t \, dX. \tag{25}$$

This may be rearranged to give the energy as

$$E = \frac{\int \Psi H \Psi_t \, dX}{\int \Psi\Psi_t \, dX} \tag{26}$$

or

$$E = \frac{\int f E_{\text{loc}} \, dX}{\int f \, dX}. \tag{27}$$

The equivalent Monte Carlo expression, for equally weighted samples based on f, gives the energy as the average of local energies,

$$E = \frac{\sum \frac{H\Psi_T}{\Psi_T}}{\sum 1} = \frac{\sum E_{\text{loc}}}{\sum 1}. \tag{28}$$

The first applications in diffusion Monte Carlo were made for the nodeless ground state of the molecular ion H_3^+ [39]. The effect was a substantial improvement in accuracy from an energy of $-1{\cdot}3414 \pm 0{\cdot}0043$ hartrees in an earlier calculation to $-1{\cdot}3439 \pm 0{\cdot}0002$ hartrees in a similar calculation using importance sampling. The statistical error is reduced by a factor of about 20 and any systematic error is presumed to be similarly reduced.

The nodes of the trial function become the fixed nodes of the wavefunction Ψ which is the exact solution for the Schrödinger equation for boundary conditions corresponding to the fixed nodes. As for simple diffusion with fixed nodes the energy determined

is an upper bound to the true energy. Trial wavefunctions from any source may be used for importance sampling but they must have the appropriate symmetry for the desired electronic state. Since no analytic integrations are required, the functional form is not restricted to integrable expressions such as those of analytic variational wavefunctions. The inter-electronic distances r_{ij} may be included explicitly. Adjustable parameters in the trial wavefunction may be optimized without integrations.

Early calculations for molecular systems with nodes include the systems H–H–H [40, 41], LiH [42], H_2O [10], CH_4 [11], and HF [12]. The trial wavefunctions for most of these calculations were taken from relatively simple analytic variational calculations, in most cases from calculations at the self-consistent field (SCF) level. The typical function was that for the 10-electron system methane [11] with an SCF trial function given by the product of the SCF function, which is a ten-by-ten determinant made up of two five-by-five determinants, and a Bijl or Jastrow function for each pair of electrons,

$$J = \exp\left[\frac{br_{ij}}{1 + cr_{ij}}\right]. \tag{29}$$

The values of b and c were specified as 1/2 for pairs of electrons with opposite spins and as 1/4 for pairs with identical spins. This avoids infinities in the local energy for two electrons at the same position. The Jastrow functions incorporate the main effects of electron–electron interactions and give a significant improvement over simple SCF trial functions. More accurate, more flexible expressions are available.

6. Time-step error in DQMC

In diffusion quantum Monte Carlo the Schrödinger equation in imaginary time is a differential equation applicable to infinitesimal changes in time, position, and weight of psips. It is simulated by numerical methods using finite time steps and the results are exact only in the limit of small time-step sizes. The algorithms first used were crude and severely limited the accuracy of the calculations, but newer algorithms are much improved and time-step errors have been reduced by several orders of magnitude. The effect has been to improve greatly the accuracy of fixed-node calculations, not only in reducing time-step error directly but also in reducing statistical error by allowing calculations spanning much greater periods of time with larger step sizes.

The problems of reducing time-step error are very nearly the same as those encountered in the integration of the classical equations of motion for a single particle in a force field. In reducing time-step error several workers have drawn upon existing methods, such as the predictor-corrector method, but much of the success in reducing time-step error has evolved using techniques specific to the diffusion QMC problem.

The most obvious steps were taken by Anderson [16]. These were integration of the growth term over the length of a step to obtain for the new weight of a psip $W(\text{new}) = W(\text{old}) \exp[-(V - V_{\text{ref}})\Delta\tau]$ rather than $W(\text{new}) = W(\text{old})[1 - (V - V_{\text{ref}})\Delta\tau]$ and, for pure diffusion QMC, a correction factor to account for crossing and recrossing a nodal surface. A predictor-corrector method, in which a trial step was used to estimate the drift velocity at the end of a step so that an average drift velocity over the step could be estimated, was reasonably successful [43]. More elaborate schemes of a similar nature were developed by Rothstein and Vrbik [44] in the quest for an algorithm giving a quadratic dependence on time-step size.

One device which has proved to be surprisingly successful is the use of an acceptance or rejection criterion for moves proposed by Reynolds *et al.* [10]. A move

is selected on the basis of a random diffusion step coupled with a drift step and accepted with a probability given by the square of the ratio of the trial wavefunction at the new position to that of the trial wavefunction at the old position. This has the effect of introducing reversibility in the limit of small steps—clearly a desirable attribute—but a complete justification of the procedure for finite time steps is not available. The real justification for the procedure is its observed success in reducing error. The procedure may not be intuitively acceptable for finite time steps, but it is certainly acceptable in the limit of small steps and it works extremely well.

Other schemes for reducing time-step error involve multiple or correlated sampling and differential sampling as suggested by Garmer [45]. Multiple importance-sampling or guide functions [43] have also been used. The optimum choices of step sizes have been examined in detail [46].

The most recent algorithm, developed by Umrigar, Nightingale, and Runge [8], is clearly the most successful. It takes advantage of good trial wavefunctions constructed with special attention to satisfying the cusp conditions, includes the acceptance/rejection procedure, modifies the choice of steps to account for non-analyticities in the local energy and velocities, and eliminates the possibility of trapping in persistent configurations. The result is a method by which time-step error is made nearly negligible for diffusion QMC with drift. It allows very large time steps without significant error, and the calculation efforts required for very high accuracy are correspondingly reduced.

Comparisons of time-step errors for old and new algorithms can be made with the aid of figures 5 and 6. In figure 5 the effect of time-step size on calculated energy is shown for the H ^2P_x system using the simplest of diffusion algorithms and using a first modification. In figure 6 a similar plot illustrates in the case of Be the time-step error for a basic algorithm and the reduction in time-step error for the advanced algorithm [8] described above. The changes in energy and time scales from figure 5 to figure 6 should be noted. In figure 6 the time-step error at $\Delta\tau = 0{\cdot}20$ a.u. for the advanced algorithm is 0·000 10 hartrees, a factor of approximately 1500 lower than that of the simple algorithm.

7. Applications to simple atoms and molecules

The Be atom has served as an excellent sample problem for testing fixed-node procedures. The total energy is accurately known from spectroscopic measurements of the energy required for the removal of two electrons together with accurate calculations and measurements of the energy of the helium-like ion Be^{++}. Analytic variational calculations for Be are some of the most accurate analytic variational calculations available. Thus, there are very good energies for comparisons.

The most accurate fixed-node QMC calculations for Be are those by Umrigar *et al.* [8] using the advanced time-step algorithm described above. They obtained a non-relativistic energy of $-14{\cdot}667\,18 \pm 0{\cdot}000\,03$ hartrees. The lowest-energy analytic variational calculation is that by Olsen and Sundholm [47, 48] who used a 650 000-determinant multiconfiguration wavefunction to obtain a non-relativistic total energy of $-14{\cdot}665\,57$ hartrees. A double extrapolation to the limits of an infinitely large basis set and an infinite number of determinants yields an energy of $-14{\cdot}667\,37 \pm 0{\cdot}000\,03$ hartrees. The corresponding 'experimental' value is a non-relativistic energy of $-14{\cdot}667\,375 \pm 0{\cdot}000\,025$ hartrees, obtained from the measured relativistic value of $-14{\cdot}669\,331$ hartrees [49], corrected by $+0{\cdot}001\,956 \pm 0{\cdot}000\,025$ hartrees to remove the effects of mass polarization, relativity, and the Lamb shift. These values are listed in table 1.

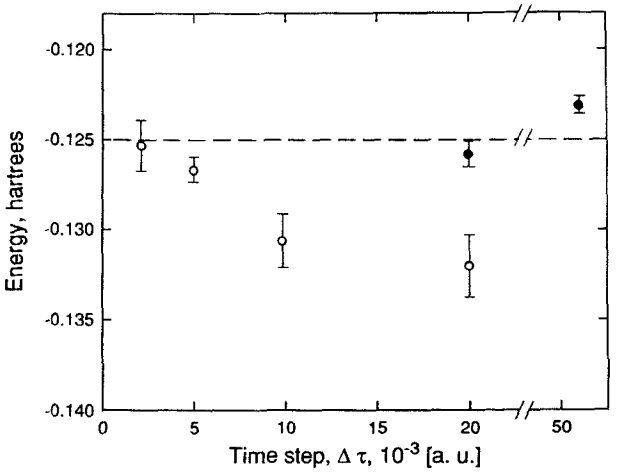

Figure 5. Illustration of time-step error in early calculations of the energy of the atom H ^2P_x. Open circles: simple algorithm. Filled circles: algorithm modified to reduce time-step error. From Anderson [43].

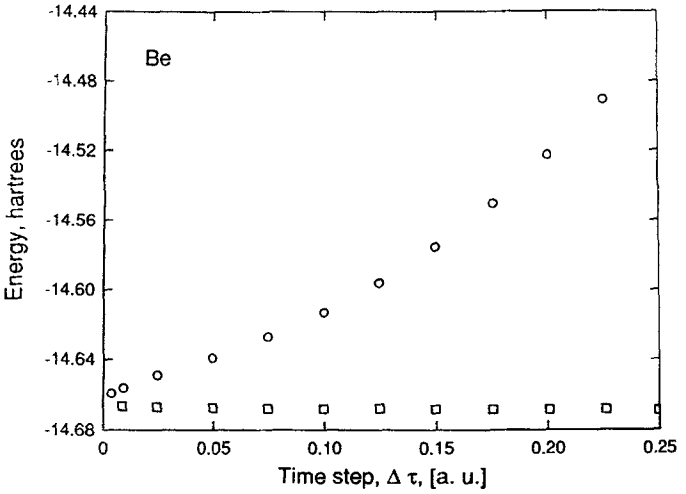

Figure 6. Illustration of the near elimination of time-step error in fixed-node calculations for the Be atom. Open circles: simple algorithm. Open squares: advanced algorithm. From Umrigar, Nightingale, and Runge [8].

Table 1. Comparisons of calculated and measured energies for Be.

Authors (date) notes	Energy (hartrees)
Umrigar, Nightingale, and Runge [8] (1993)	
fixed-node DQMC	−14·667 18 ± 0·000 03
Olsen and Sundholm [47, 48] (1991)	
analytic variational	
650 000-determinant multiconfiguration	−14·665 57
extrapolated to limit of large basis set	
and number of configurations	−14·667 37 ± 0·000 03
Holmström and Johansson [49] (1969)	
measurement of ionization potential	
together with calculated Be^{++}	
giving experimental energy	−14·669 331
'corrected' to non-relativistic	−14·667 375 ± 0·000 025

As may be seen in table 1 the energy given by the fixed-node quantum Monte Carlo calculation for Be lies +0·001 61 ± 0·000 03 below the lowest-energy variational result and only +0·000 19 ± 0·000 03 above the corresponding non-relativistic experimental value. The doubly-extrapolated variational result and the experimental value are in excellent agreement. The node-location error in the QMC calculation has been reduced to the very small value of +0·000 19 ± 0·000 03 hartrees by the use of the very accurate compact trial wavefunction obtained from careful optimization. The success of the fixed-node QMC calculation illustrates such calculations can compete with analytic variational calculations even in the case of one-centre systems for which analytic variational calculations are extremely accurate.

The LiH molecule is another species which has received much attention in QMC calculations as well as analytic variational calculations. The spectroscopy and energetics of the molecule are well known and have been reviewed recently by Stwalley and Zemke [50]. More than twenty different QMC calculations of the several types have been made for LiH and most of these are fixed-node calculations. We list them all in table 2 and include for completeness other types of QMC calculations for LiH. The various calculations were undertaken for the investigation of several different questions—questions in regard to time-step error, trial functions properly specifying node locations, released-node techniques, the incorporation of relativistic effects, GFQMC algorithms, model Hamiltonians, and energy derivatives—as well for the accurate determination of the energy of the molecule.

Calculations have been carried out for LiH at an internuclear distance of 3·015 bohrs with node locations specified by several different trial functions. The lowest-energy accurate fixed-node results are those given in [56], [58], [64],[65], and [71] with typical non-relativistic energies of approximately −8·0700 ± 0·0004 hartrees. The exact value for the non-relativistic energy is estimated to be −8·07021 hartrees. The errors resulting from inexact node locations appear to be about 0·0002 hartrees for the best trial wavefunctions used. The statistical uncertainty in the calculations is similar in size to the fixed-node error and this prevents a useful comparison of the accuracies of the node structures used. The difference, if any, in the fixed-node error for a single-determinant function is difficult to distinguish from that for four-determinant MCSCF functions. Nevertheless, it seems likely that a much more accurate trial wavefunction, like that used for Be as described above, will be found useful.

Table 2 (part 1). Quantum Monte Carlo calculations for LiH.

Authors (date) notes (internuclear distance, bohrs)	*Energy (hartrees)
Moskowitz, Schmidt, Lee, and Kalos [51] (1982)	
fixed-node, DQMC with time-step error	$-8{\cdot}0724 \pm 0{\cdot}0006$
Reynolds, Ceperley, Alder, and Lester [10] (1982)	
fixed-node DQMC with time-step error	$-8{\cdot}067 \pm 0{\cdot}002$
Ceperley [52] (1983)	
fixed-node GFQMC	$-8{\cdot}066 \pm 0{\cdot}004$
Handy [53] (1984)	
See [56]	
Oskuz [54] (1984)	
fixed-node (approximate) DQMC ($R = 3{\cdot}000$)	$-8{\cdot}075 \pm 0{\cdot}019$
Ceperley and Alder [22] (1984)	
fixed-node GFQMC	$-8{\cdot}067 \pm 0{\cdot}001$
released-node GFQMC	$-8{\cdot}071 \pm 0{\cdot}001$
Wells [55] (1985)	
fixed-node DQMC with correlated walks	$-8{\cdot}059 \pm 0{\cdot}003$
Harrison and Handy [56] (1985)	
fixed-node DQMC	$-8{\cdot}0697 \pm 0{\cdot}0003$
Moskowitz and Schmidt [26] (1986)	
fixed-node GFQMC ($R = 3{\cdot}010$)	$-8{\cdot}071 \pm 0{\cdot}002$
also other distances	
Schmidt and Moskowitz [57] (1986)	
See [26]	
Barnett, Reynolds, and Lester [58] (1987)	
fixed-node DQMC	$-8{\cdot}0700 \pm 0{\cdot}0004$
Rothstein, Patil, and Vrbik [46] (1987)	
fixed-node DQMC	
several algorithms	
East, Rothstein, and Vrbik [59] (1988)	
fixed-node DQMC	$-8{\cdot}0667 \pm 0{\cdot}0006$
DePasquale, Rothstein, and Vrbik [60] (1988)	
fixed-node DQMC	
with extrapolation for time-step	$-8{\cdot}0673 \pm 0{\cdot}0014$
Vrbik, DePasquale, and Rothstein [61] (1988)	
fixed-node DQMC with	
relativistic correction as a perturbation	

*Non-relativistic, for internuclear distance $R = 3{\cdot}015$ bohrs unless noted.

The two most accurate released-node calculations for LiH, giving energies without node-location error, are those by Caffarel and Ceperley [68] giving $-8{\cdot}0700 \pm 0{\cdot}0002$ hartrees and by Chen and Anderson [71] giving $-8{\cdot}070\,21 \pm 0{\cdot}000\,05$ hartrees. These are in agreement with the estimated true energy of $-8{\cdot}070\,21$ hartrees within their statistical uncertainties.

The lowest-energy analytic variational calculation for LiH at 3·015 bohrs is that by Handy *et al.* [72] with a trial function of 132 015 determinants obtained from single and double substitutions with 168 basis functions yielding an expectation value of $-8{\cdot}069\,04$ hartrees. This energy is 0·0012 hartrees above the estimated exact non-relativistic energy. The difference is more than a factor of ten greater than the uncertainty in the best released-node calculation.

(One advantage of 'exact' calculations is illustrated by the record for LiH. The estimated exact value of the energy reported by Handy *et al* [72] for comparison with

Table 2 (part 2). Quantum Monte Carlo calculations for LiH.

Authors (date) notes (internuclear distance, bohrs)	*Energy (hartrees)
Sun, Reynolds, Owen, and Lester [62] (1989)	
fixed-node DQMC	
varied correlation functions	-8.071 ± 0.002
Carlson, Moskowitz, and Schmidt [63] (1989)	
two-electron GFQMC	
with model Hamiltonian-dissociation energy	
Vrbik, Legare, and Rothstein [64] (1990)	
fixed-node DQMC	
to obtain derivatives of operators	-8.0670 ± 0.0004
Caffarel, Gaeda, and Ceperley [65] (1991)	
fixed-node DQMC	-8.0691 ± 0.0006
released-node DQMC	-8.070 ± 0.001
Bueckert, Rothstein, and Vrbik [66] (1992)	
VQMC with four configurations	-8.0558 ± 0.0005
>100 parameters	
Bueckert, Rothstein, and Vrbik [67] (1992)	
VQMC	-8.0669 ± 0.0007
with estimate of relativistic correction	
Caffarel and Ceperley [68] (1992)	
fixed-node DQMC	-8.0680 ± 0.0006
released-node DQMC	-8.0700 ± 0.0002
Subramaniam, Lee, Schmidt, and Moskowitz [69] (1992)	
fixed-node GFQMC	-8.0699 ± 0.0010
Vrbik and Rothstein [70] (1992)	
fixed-node DQMC	
variation of ground state-energy with geometry	
Chen and Anderson [71] (1994)	
released mode GFQMC	$-8.070\,21 \pm 0.000\,05$

*Non-relativistic, for internuclear distance $R = 3.015$ bohrs unless noted.

their upper bound was slightly in error. At $-8.070\,49$ hartrees that estimated value was inconsistent with the result of $-8.0700 \pm 0.000\,2$ hartrees determined in the released-node calculations by Caffarel and Ceperley [71] and these authors corrected the earlier estimate to obtain the estimated exact value of $-8.070\,23$ hartrees. This is a case in which the higher accuracy and known uncertainty of a QMC calculation resulted in the correction of an 'experimental' value.)

For the methane molecule fixed-node DQMC calculations by Garmer and Anderson [11] gave a total electronic energy 30 kcal mole^{-1} below the lowest-energy analytic variational calculations and only 4.8 ± 1.4 kcal mole^{-1} above the experimental non-relativistic energy. The QMC calculations recovered 97% of the correlation energy. A comparison of several relevant calculations for methane is given in table 3.

The methane calculations were carried out using a single-determinant trial function of double-zeta STO quality obtained from an analytic fit to the function given by a Hartree–Fock calculation with a standard Gaussian basis set. The double-zeta function was found superior to a single-zeta function which gave an energy approximately 10 kcal mole^{-1} higher. In each case the single-determinant function was multiplied by Jastrow functions for each possible pair of electron–electron interactions to produce a partial correlation of electron positions without affecting node locations. As may be

Table 3. Comparison of theoretical predictions and experimental measurement for methane*.

Method	Total energy (hartrees)	Correlation energy (%)	Energy above exact (kcal mol^{-1})	Reference
Hartree–Fock				
Minimal (SZ) STO's	−40·1212			[73]
Double-zeta STO's	−40·1728		214·1	[11]
Estimated limit	−40·219	0	185·1	[74]
Analytic variational extended basis CI	−40·4584	81	34·9	[75]
Quantum Monte Carlo fixed-node QMC	−40·481 ± 0·002	97	4·8	[11]
Experimental (non-relativistic)	−40·514 ± 0·002	100	0·0	[74, 76]

*$R_{C-H} = 2{\cdot}05$ bohrs.

Table 4. [a,b]A sampling of calculations for the reaction $F + H_2 \rightarrow + H$.

Authors	Date	Type	$E(F + H_2)$ Total (hartrees)	$E(F + H_2) - E$ (exact) Error (kcal mol^{-1})	E (saddle) $- E(F + H_2)$ Barrier (kcal mol^{-1})	$E(HF + H) - E(F + H_2)$ Exoergicity (kcal mol^{-1})
[77] BPOS	1971	analyt. var.	−100·5425	227·9	5·72	18·9
[78] BOPS	1972	analyt. var.	−100·5620	215·7	1·66	34·5
[79] BT	1987	analyt. var.		[c]160·0	4·50	28·8
[80] KSW	1991	analyt. var.	−100·7122	121·5	3·17	27·9
[81] USL9	1977	analyt. var.	−100·7125	121·3	3·93	32·6
[82] WKW	1992	analyt. var.	−100·7874	74·3	1·78	31·6
[83] SSBT	1985	analyt. var.	−100·7876	74·2	3·69	33·7
[84] FBS	1984	analyt. var.	−100·7892	73·2	3·24	33·7
[81] USL8	1977	analyt. var.	−100·7975	68·0	6·03	28·7
[85] BWLTJ	1988	analyt. var.		[c]52·0	2·63	31·6
[86] Scu	1991	analyt. var.	−100·8290	48·2	2·05	31·6
[12] GA	1988	FN-QMC	−100·8923	8·5	4·5 ± 0·6	29·0
[87] exact			−100·9058	0·0		31·6

[a] Includes only calculations for which total electronic energies have been reported.
[b] See original papers for effects of various theoretically justified corrections.
[c] Approximate.

seen in table 3 the expectation value for the energy of the double-zeta function is 30 kcal mole^{-1} above the Hartree–Fock limit. Use of the Jastrow factors lowers the expectation value by about 75 k cal mole^{-1}. The additional lowering to 4·8 ± 1·4 kcal mole^{-1} above the experimental total energy results from exact solution of the Schrödinger equation within the restrictions of the fixed-node boundary conditions.

The difficulties in making accurate predictions of the potential energy surface for the reaction $F + H_2 \rightarrow HF + H$ illustrate some of the problems which occur for QMC calculations as well as those which occur for analytic variational calculations. The reaction is of special theoretical interest since it is one of the simplest exothermic

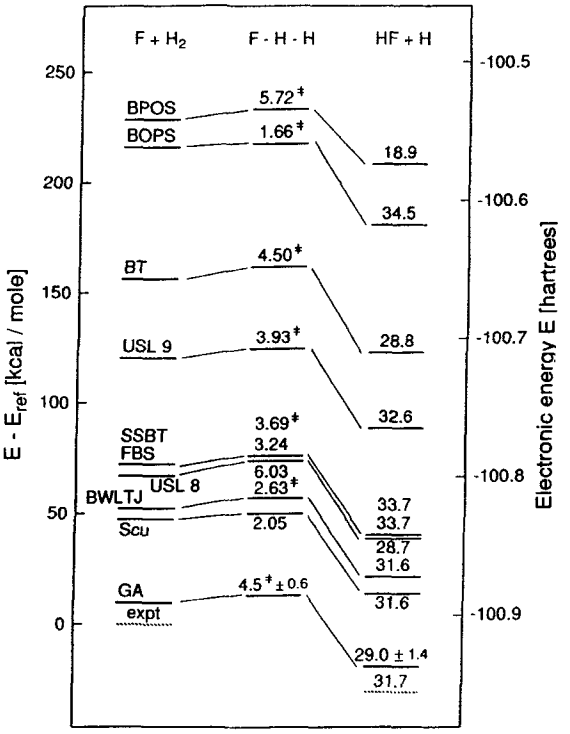

Figure 7. Electronic energies for the F–H–H system as given by several calculations. Barrier heights and exothermicities are indicated in kcal mol^{-1}. See table 4. BPOS-Bender, Pearson, O'Neill, and Schaefer, 1971, [77]. BOPS-Bender, O'Neill, Pearson, and Schaefer, 1972, [78]. BT-Bauschlicher and Taylor, 1987, [79]. KSW (not shown)-Knowles, Stark, and Werner, 1991, [80]. USL8 and USL9-Ungemach, Schaefer, and Liu, 1977 [81]. WKW (not shown)-Wright, Kolbuszewski, and Wyatt, 1992, [82]. SSBT-Schwenke, Steckler, Brown, and Truhlar, 1985, [83]. FBS-Frisch, Binkley, and Schaefer, 1984, [84]. BWLTJ-Bauschlicher, Walch, Langhoff, Taylor and Jaffe, 1988, [85]. Scu-Scuseria, 1991, [86]. GA-Garmer and Anderson (QMC), 1988, [12].

reactions and since there is a wealth of experimental data for it available from a variety of experiments. Excellent reactive scattering calculations have been made for several approximate potential surfaces.

The results of calculations of all types to determine the barrier height for the reaction of F with H_2 by are listed in table 4 and plotted in figure 7. For each set of calculations the expectation values of the energies are shown (left) for separated reactants F + H_2, (centre) for the saddle-point configuration F–H–H or a nearby point, and (right) for separated products HF + H. The energy of the saddle point relative to reactants and that of products relative to reactants are indicated for each set of calculations. The estimated exact non-relativistic total energies for reactants and products, available from experiment, are indicated by dashed lines. The experimental activation energy is in the range of 0·7 to 1·3 kcal mole^{-1}. An experimental barrier height is, of course, not directly available. It is probably in the range of 1·5 to 3·0 kcal mole^{-1}, but it might be outside that range.

The general trend in total energies for analytic variational calculations is toward lower energies at later dates, but the relative value at the saddle point—the barrier

height—is highly variable. The lowest-energy analytic variational calculation is the coupled-cluster calculation by Scuseria [86] yielding a barrier height of 2·05 kcal mole^{-1} and an energy for reactants 48·2 kcal mole^{-1} above the exact total energy.

The fixed-node QMC calculations by Garmer and Anderson [12] gave a barrier height of 4·5 ± 0·6 kcal mole^{-1} and an energy for reactants only 8·5 kcal mole^{-1} above the exact energy. The node structure for the calculations was that of a high quality single-determinant function obtained by fitting the results of a standard Gaussian SCF calculation. If the node structure for such a simple function is sufficiently accurate to give an error of only 8·5 kcal mole^{-1}, one might expect simple MCSCF functions and better to five extremely low node-location errors. For systems like F–H–H this possibility remains open.

The barrier height of 4·5 ± 0·6 kcal mole^{-1} for collinear reaction of F with H_2 indicated by the QMC calculations is probably too high to be compatible with experimental results. But, it might be entirely correct. The favoured reaction path may pass through a bent F–H–H configuration. The QMC results for a bent configuration suggested the barrier for non-linear reaction may be somewhat lower than for collinear reaction, and this feature has now been found in several analytic variational calculations.

The chief problems for the analytic variational calculations are the large errors in total energy and the uncertainties introduced by these errors when relative values of energies are calculated. Unless experimental data for similar situations is available one cannot judge in a particular case whether such errors in total energies cancel when relative values are calculated.

The chief problems for the fixed-node QMC calculations are similar. Unless experimental data for similar situations is available one cannot judge whether the node-location errors, even though smaller, will cancel when relative values are calculated.

For QMC calculations there is much less prior experience than for analytic variational calculations. A body of data is slowly being accumulated, but it is still too early to make any general conclusions. For all-electron calculations the nodal surface in the core region is likely to be greatest source of node-location error, and one might expect that cancellation of errors would be nearly complete. Further investigation is required.

8. Effective potentials and effective Hamiltonians

Quantum Monte Carlo calculations, like analytic variational calculations, can be considerably simplified by the use of effective potentials to replace core electrons tightly packed around nuclei. One expects and one hopes that, as in analytic variational calculations with effective potentials or with frozen core basis sets, the energies of the core electrons and their effect on valence electrons will be almost exactly cancelled in subtracting to obtain relative energies for nearly identical systems. Since the energies of core electrons in heavy atoms are usually very much greater than the energies of valence electrons, including core electrons in QMC calculations is very much more expensive computationally when statistical error in the total energy must be reduced. The advantages of eliminating core electrons are large in proportion to the number of core electrons eliminated.

The effective potentials normally used in analytic variational calculations are non-local potentials which involve angular projection operators which cannot be simply transferred into QMC calculations. In the earliest QMC calculations to use effective

potentials Hurley and Christiansen [88] avoided this difficulty with the use of local potentials V_{loc} defined in terms of a trial wavefunction,

$$V_{\text{loc}} = \frac{U^{\text{REP}}\Psi_t}{\Psi_t}, \tag{30}$$

where U^{REP} is a conventional relativistic (or non-relativistic) effective potential. The use of effective potentials is, by its nature, not exact and introduces systematic errors which, in most treatments thus far, have been found to be small. In later work non-local effective potentials [89–91] have been used with success as have their more-complex counterparts, effective Hamiltonians. These too introduce systematic errors of finite size, but the errors are not easily analysed and not easily understood. For that reason it is difficult to make judgements about the relative merits of the several methods. Greater success in reproducing experimental observations might simply be the result of greater flexibility in more elaborate treatments. Questions of the relative utility and reliability of effective potentials and effective Hamiltonians have been discussed in some detail by Bachelet *et al.* [91] and by Christiansen [92].

A list of studies using effective potentials, model potentials, effective Hamiltonians, and related devices is given in table 5. The typical first calculations for any research group are those to determine an electron affinity of a species such as Li, obtained by calculations of the energies of one and two electrons, respectively, in the field of an Li^+ ($1s^2$) core potential, and subtraction of the energies. Several of these are listed in the table. Larger numbers of electrons are included in calculations of the electron affinities of species such as Cl atoms using neon core potentials and of the energies of multiple states of atoms such as Al, Sc, and Fe. Still larger numbers of electrons are included in treatments of solid silicon as a collection of 64 Si atoms with a total of 256 valence electrons [14].

The results obtained by Christiansen [92] for the transition metal atoms Sc and Y illustrate the accuracies obtained in fixed-node diffusion quantum Monte Carlo calculations using simple effective potentials. In these calculations Christiansen used previously determined relativistic effective potentials for Sc and Y with 11 valence electrons to determine energies for the ^2D and ^2F states of these atoms. The fixed-node calculations used simple SCF trial functions incorporating Jastrow electron–electron correlation functions and optimized for the ground states. The computed excitation energies for the transitions between the two states were 1·5(3) and 1·4(2) eV, respectively, for Sc and Y. These may be compared to the experimental values of 1·43 and 1·36 eV, respectively.

In further investigations of the accuracies of QMC calculations using effective potentials Lao and Christiansen [107] calculated the valence correlation energy for Ne and found excellent agreement with previous full-CI benchmark calculations. They recovered 98 to 100% of the valence correlation energy and could detect no significant error due to the effective potential approximation.

Overall, the use of effective potentials, model potentials, pseudopotentials, and pseudo-Hamiltonians of the several types has been found extremely useful in extending the range of fixed-node QMC calculations. To the extent to which the calculations can be checked for accuracy, by comparison of results with those of experiments and otherwise, there is every indication that such fixed-node QMC calculations are as accurate or more accurate than any other type of calculation currently available.

Table 5. Fixed-node QMC calculations with effective potentials.

Authors (date)	Species
Hurley and Christiansen [88] (1987) effective potentials	Li/Li^- K/K^-
Hammond, Reynolds, and Lester [93] (1987) effective potentials	Li/Li^+ Na/Na^+ Mg/Mg^+ NaH/Na + H
Christiansen [94] (1988) effective potentials	Be (three states)/Be^+
Cristiansen and LaJohn [95] (1988) effective potentials	Mg/Mg^+
Yoshida and Iguchi [96] (1988) model potentials	Mg/Mg^+ Ca/Ca^+ Sr/Sr^+
Yoshida, Mizushima, and Iguchi [97] (1988) model potentials	Cl/Cl
Carlson, Moskowitz, and Schmidt [98] (1989) model Hamiltonians	Li/LiH Li_2/2Li
Christiansen [99] (1989) effective potentials	Al (two states)/Al^+
Bachelet, Ceperley, and Chiocchetti [91] (1989) pseudo-Hamiltonians	Na_2/Na/Na^-/Na^+ also Mg, Si Cl dimers and ions
Christiansen [100] (1990) effective potentials	Al (three states)/Al^+
Shirley, Martin, Bachelet, and Ceperley [101] (1990) pseudopotentials	Na, K, Si ions, dimers, dimer ions
Yoshida and Iguchi [102] (1990) model potentials	Ca/Ca^+ Br/Br^-
Foulkes and Schluter [89] (1990) pseudopotentials	indirect evaluations
Li, Ceperley, and Martin [14] (1991) pseudo-Hamiltonians	solid Si/Si
Mitas, Shirley, and Ceperley [103] (1991) non-local pseudopotentials	Si_2/Si/Si^-/Si^+/Si^{++} Cu/Cu^+/Cu^-
Christiansen [92] (1991) effective potentials	Sc (two states) Y (two states)
Shirley, Mitas, and Martin [104] (1991) partitioning/quasi-particle potentials	Be/Be^+ (four states) Na/Na^+ (four states) Sc/Sc^+ (four states)
Mitas [105] (1992) pseudopotentials	Fe (two states)
Flad, Savin, and Preuss [90] (1992) pseudopotentials	Be/Be^+ also Mg, Ca, Sr, Ba Li, Na, K, mixed dimers
Schrader, Yoshida, and Iguchi [106] (1992) model potentials	PsCl/Ps + Cl
M. Lao and P. A. Christiansen [107] (1992) effective potentials	Ne
Schrader, Yoshida, and Iguchi [108] (1993) model potentials	PsF/Ps + F PsCl/Ps + Cl PsBr/Ps + Br
Belohorec, Rothstein, and Vrbik [109] (1993) related to pseudopotentials	CuH (several states)

9. Applications to larger systems

The extension of QMC methods to problems of a large number of electrons has taken place mainly in the area of condensed matter systems. Standard approaches to condensed matter systems have often given good agreement with experimental measurements of structural properties, but they have very often failed in the prediction binding energies of crystalline materials. There is much current interest in predictions of the energetics of such materials as well as their electronic properties. There is also much interest in predicting structures, energetics, and related properties of the surfaces of solid materials. Advances in the computation of molecular dynamics have created a very large demand for accurate potential energy surfaces for systems with large numbers of electrons.

One of the first applications of general QMC techniques to a problem in condensed matter was made by Fahy, Wang, and Louie [110] in variational QMC calculations for carbon (diamond), carbon (graphite), and silicon. They used pseudopotentials together with trial wavefunctions in the form of Slater determinants multiplied by Bijl–Jastrow factors. Cell sizes of up to 216 electrons (corresponding to 54 carbon atoms) were used. Their results for several basic properties of carbon (diamond) and of silicon are listed in table 6 along with experimental values. It may be seen that the agreement with experiment is excellent.

Variational QMC calculations are the starting point for fixed-node QMC calculations. If the variational QMC calculations give good results one should expect even better from fixed-node calculations. This is indeed what has been observed in fixed-node calculations for solid silicon. Li, Ceperley, and Martin [14] made variational QMC calculations for silicon using pseudo-Hamiltonians as well as fixed-node QMC calculations using the same Hamiltonians. Some of their results are listed in table 6. It may be seen the fixed-node QMC results are in excellent agreement with experimental measurements. The variation of cohesive energy with lattice constant for both sets of calculations is shown in figure 8. In their variational calculations Li *et al.* [14] found a larger difference from experiment than Fahy *et al.* [110] and this suggests variational QMC calculations for these systems may be less accurate than supposed. There is no suggestion of any problem with the extremely accurate predictions of the fixed-node QMC calculations.

In related work Natoli, Martin, and Ceperley [111] made fixed-node calculations of the crystal structure of atomic hydrogen. They determined energies for five different crystal structures (body-centred cubic, simple cubic, simple hexagonal, diamond, β-Sn) with varied densities using a range of system sizes from 8 to 432 atoms with and without fixed protons. The results show that low-coordination structures, particularly the diamond structure, are favoured at pressures below about 3 Mbars.

10. Future directions

As noted above, the demand for accurate potential energy surfaces for condensed matter systems is great. A similar demand exists for other large molecular systems, especially for biomolecules, protein structures and enzymes, with and without surrounding solvent molecules. We expect the number of applications attempted with quantum Monte Carlo methods to increase and the number of successful applications to increase as well.

For systems of up to about ten electrons it seems likely that 'exact' quantum Monte Carlo methods—those which treat the node problem exactly— will within a relatively short time replace fixed-node calculations. The fixed-node quantum Monte Carlo

Table 6. Some QMC calculations of the energies and structures of solid materials.

System Calculation	Lattice Constant (Å)	Atomic Energy (eV/atom)	Solid Energy (eV/atom)	Cohesive Energy (eV/atom)
Carbon (diamond)				
VQMC, pseudopotential [110]	3·54(3)	−147·93(3)	−155·38(6)	7·45(7)
Experiment[a]	3·567			7·37
Silicon				
VQMC, pseudopotential [110]	5·40(4)	−103·42(3)	−108·23(6)	4·81(7)
VQMC, pseudo-Hamiltonian [14]	5·42(2)	−103·35(3)	−107·73(2)	4·38(4)
FN-QMC, pseudo-Hamiltonian [14]	5·45(2)	−103·56(2)	−108·07(2)	4·51(3)
Experiment[b]	5·430			4·63(8)

[a] See list in [110].
[b] See lists in [110] and [14].

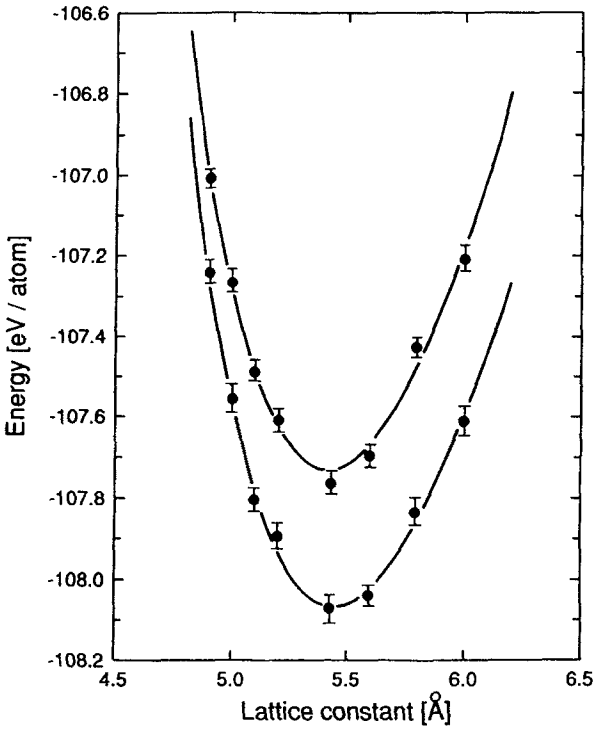

Figure 8. Calculated total energy of silicon as a function of the lattice constant. Upper set of points: variational QMC. Lower set of points: fixed-node DQMC. The curves are fits of the Murnaghan equation of state to the calculated points. From Li, Ceperley, and Martin [14].

method will find its principle applications in calculations for the large systems. The major advances will come with faster machines and very much better trial wavefunctions, and perhaps a breakthrough in separating the determinants of trial wavefunctions into significant and insignificant parts.

Acknowledgments

Support of this work by the National Science Foundation and the Office of Naval Research is gratefully acknowledged. The author is indebted to the Hamboldt Foundation for an award facilitating this work.

References

[1] ANDERSON, J. B., 1992, *J. chem. Phys.*, **96,** 3702.
[2] DIEDRICH, D. L., and ANDERSON, J. B., 1992, *Science*, **258,** 786.
[3] ANDERSON, J. B., TRAYNOR, C. A., and BOGHOSIAN, B. M., 1993, *J. chem. Phys.*, **99,** 345.
[4] CAFFAREL, M., and CEPERLEY, D. M., 1992, *J. chem. Phys.*, **97,** 8415.
[5] BHATTACHARYA, A., and ANDERSON, J. B., 1994, *Phys. Rev.* A, **49,** 2441.
[6] TRAYNOR, C. A., Anderson, J. B., and BOGHOSIAN, B. M., 1991, *J. chem. Phys.*, **94,** 3657.
[7] ANDERSON, J. B., 1994, *Quantum Mechanical Electronic Structure Calculations with Chemical Accuracy*, edited by S. R. Langhoff (Dordrecht: Kluwer).
[8] UMRIGAR, C. J., NIGHTINGALE, M. P., and RUNGE, K. J., 1993, *J. chem. Phys.*, **99,** 2865.
[9] MITAS, L., 1994, *Phys. Rev.* A, **49,** 4411.
[10] REYNOLDS, P. J., CEPERLEY, D. M., ALDER, B. J., and LESTER, W. A., 1982, *J. chem. Phys.*, **77,** 5593.
[11] GARMER, D. R., and ANDERSON, J. B., 1987, *J. chem. Phys.*, **86,** 4025.
[12] GARMER, D. R., and ANDERSON, J. B., 1987, *J. chem. Phys.*, **87,** 7237.
[13] MITAS, L., and MARTIN, R. M., 1994, *Phys. Rev. Lett.*, **72,** 2438.
[14] Li, X.-P., CEPERLEY, D. M., and MARTIN, R. L., 1991, *Phys. Rev.* B, **44,** 10929.
[15] ANDERSON, J. B., 1975, *J. chem. Phys.*, **63,** 1499.
[16] ANDERSON, J. B., 1976, *J. chem. Phys.*, **65,** 4121.
[17] WIGNER, E. P., 1932, *Phys. Rev.*, **40,** 749.
[18] METROPOLOS, N., and ULAM, S., 1949, *J. Am. statist. Ass.*, **44,** 335.
[19] KING, G. W., 1951, *Proceedings, IBM Computation Seminar*, Endicott, New York, 1949 (New York: International Business Machines Corp.), P. 92.
[20] EINSTEIN, A., 1905, *Ann. Phys.*, **17,** 549; 1906, *Ibid.*, **19,** 371.
[21] ANDERSON, J. B., TRAYNOR, C. A., and BOGHOSIAN, B. M., 1991, *J. chem. Phys.*, **95,** 7418.
[22] CEPERLEY, D. M., and ALDER, B. J., 1984, *J. chem. Phys.*, **81,** 5833.
[23] KALOS, M. H., 1962, *Phys. Rev.*, **128,** 1791.
[24] CEPERLEY, D. M., 1983, *J. comput. Phys.*, **51,** 404.
[25] SKINNER, D. W., MOSKOWITZ, J. W., LEE, M. A., WHITLOCK, P. A., and SCHMIDT, K. E., 1985, *J. chem. Phys.*, **83,** 4668.
[26] MOSKOWITZ, J. W., and SCHMIDT, K. E., 1986, *J. chem. Phys.*, **85,** 2868.
[27] KLEIN, D. J., and PICKETT, H. M., 1976, *J. chem. Phys.*, **64,** 4811.
[28] JAMES, H. M., COOLIDGE, A. S., and PRESENT, R. D., 1936, *J. chem. Phys.*, **4,** 187.
[29] KOLOS, W., and ROOTHAAN, C. C. J., 1960, *Rev. mod. Phys.*, **32,** 219.
[30] KOLOS, W., and WOLNIEWICZ, L., 1965, *J. chem. Phys.*, **43,** 2429.
[31] ANDERSON, J. B., 1979, *Int. J. quant. Chem.*, **15,** 109.
[32] BAUER, S. H., and OSSA, E., 1966, *J. chem. Phys.*, **45,** 434.
[33] BURCAT, A., and LIFSHITZ, A., 1967, *J. chem. Phys.*, **47,** 3079; KERN, R. D., and NIKA, G. G., 1971, *J. phys, Chem.*, **75,** 1615.
[34] WILSON, C. W., and GODDARD, W. A., 1972, *J. chem. Phys.*, **51,** 716.
[35] RUBINSTEIN, M., and SHAVITT, I., 1969, *J. chem. Phys.*, **51,** 2014.
[36] SILVER, D. M., and STEVENS, R. M., 1972, *J. chem. Phys.*, **59,** 3378.
[37] ANDERSON, J. B., and FREIHAUT, B. H., 1979, *J. comput. Phys.*, **31,** 425.
[38] GRIMM, R. C., and STORER, R. G., 1971, *J. comput. Phys.*, **7,** 134.
[39] MENTCH, F., and ANDERSON, J. B., 1981, *J. chem. Phys.*, **74,** 6307.
[40] MENTCH, F., and ANDERSON, J. B., 1984, *J. chem. Phys.*, **80,** 2675.

[41] BARNETT, R. N., REYNOLDS, P. J., and LESTER, W. A., 1995, *J. chem. Phys.* (in press).
[42] HARRISON, R. J., and HANDY, N. C., 1985, *Chem. Phys. Lett.*, **113,** 257.
[43] ANDERSON, J. B., 1980, *J. chem. Phys.*, **73,** 3897.
[44] VRBIK, J., and ROTHSTEIN, S. M., 1986, *Int. J. quant. Chem.*, **29,** 461.
[45] GARMER, D. R., 1989, *J. comput. Chem.*, **10,** 176.
[46] ROTHSTEIN, S. M., PATIL, N., and VRBIK, J., 1987, *J. comput. Chem.*, **8,** 412.
[47] OLSEN, J., and SUNDHOLM, D., reported in [48].
[48] MÅRTENSON-PENDRILL, A.-M., *et al.*, 1991, *Phys. Rev.* A, **43,** 3355.
[49] HOLMSTRÖM, J. E., and JOHANSSON, L., 1969, *Ark. Fys.*, **40,** 133.
[50] STWALLEY, W. C., and ZEMKE, W. T., 1993, *J. phys. Chem. Ref. Data*, **22,** 87.
[51] MOSKOWITZ, J. W., SCHMIDT, K. E., LEE, M. A., and KALOS, M. H., 1982, *J. chem. Phys.*, **77,** 349.
[52] CEPERLEY, D. M., 1983, *J. comput. Phys.*, **51,** 404.
[53] HANDY, N. C., 1984, *Faraday Symp. Chem. Soc.*, **19,** 17; see also: [56].
[54] OSKUZ, I., 1984, *J. chem. Phys.*, **81,** 5005.
[55] WELLS, B. H., 1985, *Chem. Phys. Lett.*, **115,** 89.
[56] HARRISON, R. J., and HANDY, N. C., 1985, *Chem. Phys. Lett.*, **113,** 257.
[57] SCHMIDT, K. E., and MOSKOWITZ, J. W., 1986, *J. statist. Phys.*, **43,** 1027; see also: 1986, *J. chem. Phys.*, **85,** 2868.
[58] BARNETT, R. N., REYNOLDS, P. J., and LESTER, W. A., 1987, *J. phys. Chem.*, **91,** 2004.
[59] EAST, A. L. L., ROTHSTEIN, S. M., and VRBIK, J., 1988, *J. chem. Phys.*, **89,** 4880.
[60] DEPASQUALE, M. F., ROTHSTEIN, S. M., and VRBIK, J., 1988, *J. chem. Phys.*, **89,** 3629.
[61] VRBIK, J., DEPASQUALE M. F., and ROTHSTEIN, S. M., 1988, *J. chem. Phys.*, **88,** 3784.
[62] SUN, Z., REYNOLDS, P. J., OWEN, R. K., and LESTER, W. A., 1989, *Theor. chim. Acta.*, **75,** 353.
[63] CARLSON, J., MOSKOWITZ, J. W., and SCHMIDT, K. E., 1989, *J. chem. Phys.*, **92,** 1003.
[64] VRBIK, J., LEGARE, D. A., and ROTHSTEIN, S. M., 1990, *J. chem. Phys.*, **92,** 1221.
[65] CAFFAREL, M., GAEDA, F. X., and CEPERLEY, D. M., 1991, *Europhys. Lett.*, **16,** 249.
[66] BUECKERT, H., ROTHSTEIN, S. M., and VRBIK, J., 1992, *Can. J. Chem.*, **70,** 366.
[67] BUECKERT, H., ROTHSTEIN, S. M., and VRBIK, J., 1992, *Chem. Phys. Lett.*, **190,** 413.
[68] CAFFAREL, M., and CEPERLEY, D. M., 1992, *J. chem. Phys.*, **97,** 8415.
[69] SUBRAMANIAM, R. P., LEE, M. A., SCHMIDT, K. E., and MOSKOWITZ, J. W., 1992, *J. chem. Phys.*, **97,** 2600.
[70] VRBIK, J., and ROTHSTEIN, S. M., 1992, *J. chem. Phys.*, **96,** 2071.
[71] CHEN, B., and ANDERSON, J. B., 1994 (to be published).
[72] HANDY, N. C., HARRISON, R. J., KNOWLES, P. J., and SCHAEFER, H. F., 1984, *J. phys. Chem.*, **88,** 4852.
[73] PITZER, R. M., 1967, *J. chem. Phys.*, **46,** 4871.
[74] POPLE, J. A., and BINKLEY, J. S., 1975, *Mol. Phys.*, **29,** 599.
[75] MEYER, W., 1973, *J. chem. Phys.*, **58,** 1017.
[76] VEILLARD, A., and CLEMENTI, E., 1968, *J. chem. Phys.*, **49,** 2415.
[77] BENDER, C. F., PEARSON, P. K., O'NEILL, S. V., and SCHAEFER, H. F., 1971, *J. chem. Phys.*, **56,** 4626.
[78] BENDER, C. F., O'NEILL, S. V., PEARSON, P. K., and SCHAEFER, H. F., 1972, *Science*, **176,** 1412.
[79] BAUSCHLICHER, C. W., and TAYLOR, P. J., 1987, *J. chem. Phys.*, **86,** 858.
[80] KNOWLES, P. J., STARK, K., and WERNER, H.-J., 1991, *Chem. Phys. Lett.*, **185,** 555.
[81] UNGEMACH, S. R., SCHAEFER, H. F. and LIU, B., 1977, *Faraday Discuss. Chem. Soc.*, **62,** 330.
[82] WRIGHT, J. S., KOLBUSZEWSKI, M., and WYATT, R. E., 1992, *J. chem. Phys.*, **97,** 8296.
[83] SCHWENKE, D. W., STECKLER, R., BROWN, F. B., and TRUHLAR, D., 1985, *Chem. Phys. Lett.*, **121,** 475; 1986, *J. chem. Phys.*, **84,** 5706.
[84] FRISCH, M. J., BINKLEY, J. S., and SCHAEFER, H. F., 1984, *J. chem. Phys.*, **81,** 1822.
[85] BAUSCHLICHER, C. W., WALCH, S. P., LANGHOFF, S. R., TAYLOR, P. R., and JAFFE, R. L., 1988, *J. chem. Phys.*, **88,** 1743.
[86] SCUSERIA, G. E., 1991, *J. chem. Phys.*, **95,** 7426.
[87] See [12] for a discussion of the exact value.
[88] HURLEY, M. M., and CHRISTIANSEN, P. A., 1987, *J. chem. Phys.*, **86,** 1069.

[89] FOULKES, W. M. C., and SCHLUTER, 1990, *Phys. Rev.* B, **42,** 11505.
[90] FLAD, H.-J., SAVIN, A., and PREUSS, H., 1992, *J. chem. Phys.*, **97,** 459.
[91] BACHELET, G. B., CEPERLEY, D. M., and CHIOCCHETTI, M. G. B., 1989, *Phys. Rev. Lett.*, **62,** 2088.
[92] CHRISTIANSEN, P. A., 1991, *J. chem. Phys.*, **95,** 361.
[93] HAMMOND, B. L., REYNOLDS, P. J., and LESTER, W. A., 1987, *J. chem. Phys.*, **87,** 1130.
[94] CHRISTIANSEN, P. A., 1988, *J. chem. Phys.*, **88,** 4867.
[95] CHRISTIANSEN, P. A., and LAJOHN, L. A., 1988, *Chem. Phys. Lett.*, **146,** 162.
[96] YOSHIDA, T., and IGUCHI, K., 1988, *J. chem. Phys.*, **88,** 1032.
[97] YOSHIDA, T., MIZUSHIMA, Y., and IGUCHI, K., 1988, *J. chem. Phys.*, **89,** 5815.
[98] CARLSON, J., MOSKOWITZ, J. W., and SCHMIDT, K. E., 1989, *J. chem. Phys.*, **92,** 1003.
[99] CHRISTIANSEN, P. A., 1989, *ACS Symposium Series* 394, 310.
[100] CHRISTIANSEN, P. A., 1990, *J. chem. Phys.*, **94,** 7865.
[101] SHIRLEY, E. L., MARTIN, R. M., BACHELET, G. B., and CEPERLEY, D. M., 1990, *Phys. Rev.* B, **42,** 5057.
[102] YOSHIDA, T., and IGUCHI, K., 1990, *J. chem. Phys.*, **93,** 5783.
[103] MITAS, L., SHIRLEY, E. L., and CEPERLEY, D. M., 1991, *J. chem. Phys.*, **95,** 3467.
[104] SHIRLEY, E. L., MITAS, L., and MARTIN, R. M., 1991, *Phys. Rev.* B, **44,** 3395.
[105] MITAS, L., 1992, *Computer Simulation in Condensed Matter Physics* IV, edited by D. P. Landau, K. K. Mon and H. B. Schutter (Berlin: 1992, Springer).
[106] SCHRADER, D. M., YOSHIDA, T., and IGUCHI, K., 1992, *Phys. Rev. Lett.*, **68,** 3281.
[107] LAO, M., and CHRISTIANSEN, P. A., 1992, *J. chem. Phys.*, **96,** 2162.
[108] SCHRADER, D. M., YOSHIDA, T., and IGUCHI, K., 1993, *J. chem. Phys.*, **98,** 7185.
[109] BELOHOREC, P., ROTHSTEIN, S. M., and VRBIK, J., 1993, *J. chem. Phys.*, **98,** 6401.
[110] FAHY, S., WANG, X. W., and LOUIE, S. G., 1990, *Phys. Rev.* B, **42,** 3503.
[111] MORONI, S., CEPERLEY, D. M., and SENATORE, G., 1992, *Phys. Rev. Lett.*, **69,** 3281.
[112] NATOLI, V., MARTIN, R. M., and CEPERLEY, D. M., 1993, *Phys. Rev. Lett.*, **70,** 1952.